Supplementary Information

Supplementary Fig. 1: Characterisation of the ATRX KO CD34+ cell model.

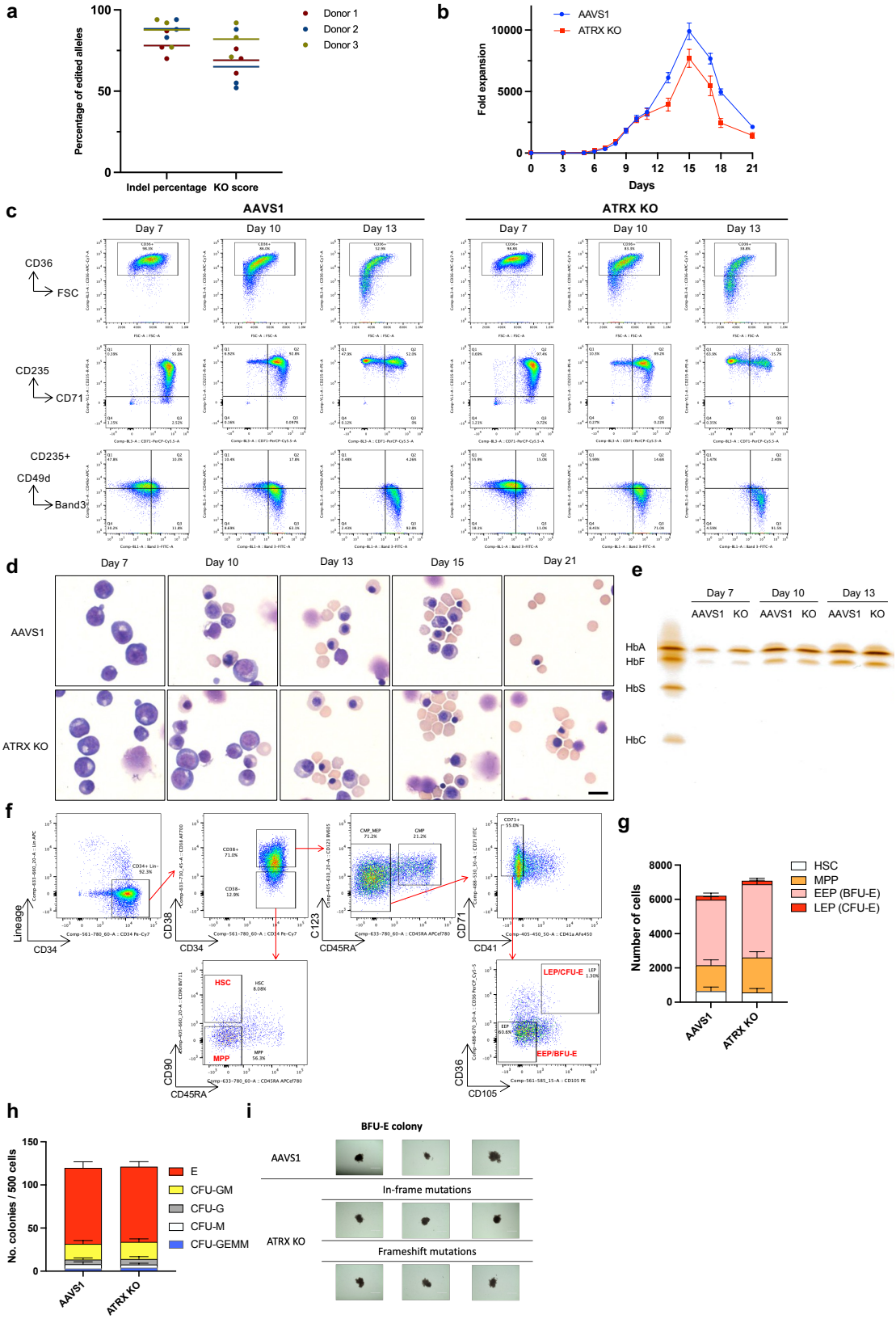

a *ATRX* knockout efficiency in day 6 differentiated cells from three independent CRISPR experiments across three donors. Efficiency was assessed using Inference of CRISPR Edits (ICE) analysis. Each dot represents one knockout experiment, horizontal lines indicate the mean, and each colour represents one donor. **b** The nucleated cell number change during differentiation showing slightly slower cell proliferation in ATRX KO cells compared to controls during differentiation (n = 3 biological replicates, data represent the mean ± SEM). **c** Representative flow cytometric analysis of erythroid cell surface markers showing ATRX KO cells exhibited similar erythroid differentiation as control AAVS1 cells. The experiment was independently repeated at least three times with similar results. **d** Representative cytospin images stained with modified Wright's stain (magnification 400x) showing similar cellular morphology changes in ATRX KO cells and control cells during erythroid differentiation. Scale bar = 10 μm. The experiment was independently repeated at least three times with similar results. **e** Haemoglobin analysis by isoelectric focusing (IEF) in cell samples at various differentiation stages. The left lane represents haemoglobin AFSC control. ATRX KO and AAVS1 samples showed similar haemoglobin expression pattern. The experiment was independently repeated at least three times with similar results. **f** Gating strategy of haematological progenitor immunophenotyping panel for examining the frequency of the progenitors and for sorting EEP. EEP ($Lin^-CD34^+CD38^+CD45RA^-CD71^+CD41A^-CD36^-CD105^-$) were sorted for CFU assays. **g** Number of sorted progenitor cells for each population in AAVS1 control and ATRX KO samples (n = 2 biological replicates). **h** Clonogenic capacity of the sorted early erythroid progenitors from *AAVS1* and *ATRX* knockout samples (n = 2 biological replicates), showing the frequency of erythroid colonies (E), granulocyte and monocyte-macrophage colonies (CFU-GM), granulocyte colonies (CFU-G), monocyte-macrophage colonies (CFU-M), and mixed granulocyte, erythroid, macrophage, megakaryocyte colonies (CFU-GEMM). **i** Morphology and size of BFU-E methocult colonies derived from AAVS1 control and ATRX KO samples, showing no difference between different genotypes. Source data are provided as a Source Data file.

Supplementary Fig. 2: Characterisation and scRNA-seq analyses in AAVS1 and ATRX KO samples.

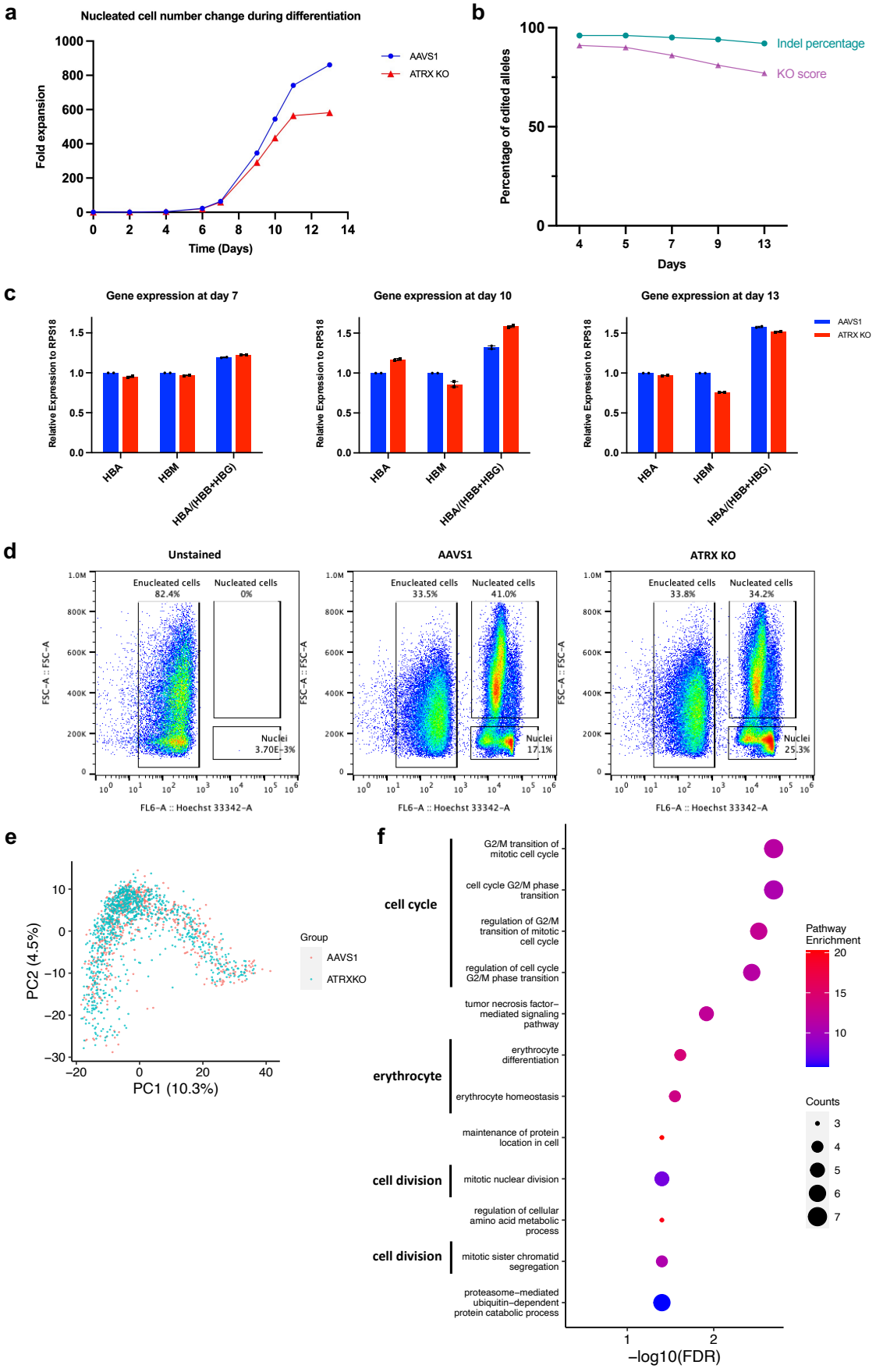

a The nucleated cell number change in AAVS1 and ATRX KO cells during erythroid differentiation until day 13. **b** ATRX knockout efficiency determined by ICE in bulk cells at various time points during differentiation. **c** RT-qPCR analysis of globin gene expression on differentiation day 7, day 10 and day 13 cells, normalised to *RPS18*. Error bars indicate SEM of two technical repeats. **d** Single-cell sorting gating for unstained control, AAVS1, and ATRX KO samples. Live nucleated cells and nuclei are both positive for the cell-permeable nuclear stain, but the sorted live nucleated cells are bigger in size than the nuclei, showing higher forward scatter (FSC) on y axis. **e** PCA plot based on HVGs. The x- and y-axes denote the top two principal components. Each dot represents a single cell, coloured by groups. **f** Dot plot of Clusterprofiler GSEA analysis of the DE genes identifying key biological processes attributed to the different transcriptome of ATRX KO cells from the AAVS1 control cells. x-axis indicates the p-value representing enrichment score; the higher the value, the more significant the enrichment. The size of the dot represents number of DE genes attributed to each GO term; the colour of the dot indicates the odds ratio of the GO term; the larger the odds ratio, the higher the relative abundance of this GO term compared with background. Source data are provided as a Source Data file.

Supplementary Fig. 3: scRNA-seq data analyses in the affected cells.

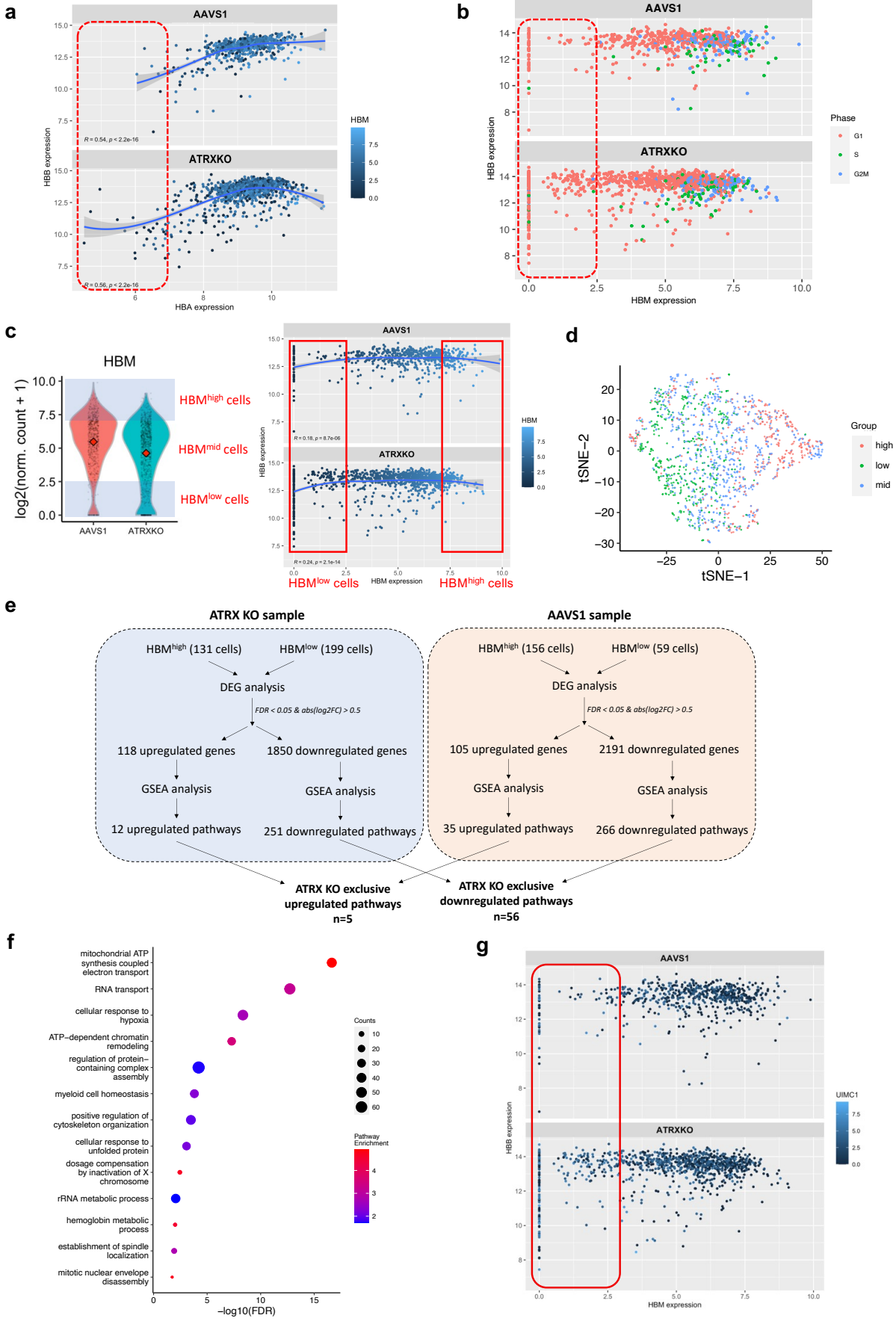

a Single-cell *HBM* and *HBB* expression in AAVS1 (top panel) and ATRX KO (bottom panel) samples, coloured by *HBM* expression level, showing a subset of ATRX KO cells expressing low *HBA*. **b** *HBM* and *HBB* expression in single cells, colour-coded by cell cycle phase, revealing the affected cells in the ATRX KO group are mostly in G1 phase. **c** Re-classification of cells based on their *HBM* expression levels: cells with *HBM* expression < 2.5 were categorised as HBM^{low}, those with *HBM* expression > 7 as HBM^{high}, and the remainder as HBM^{mid}. **d** t-SNE plots of scRNA-seq data coloured by HBM reclassification groups, depicting HBM^{low} cluster is now more separated from other cells. **e** Workflow for DEG and GSEA analysis between affected HBM^{low} and unaffected cells. DEG and GSEA analyses were performed separately in both samples and then pathways uniquely dysregulated in ATRX KO sample were identified. **f** Selected 13 downregulated pathways in the affected HBM^{low} cells. **g** Single-cell gene expression (*HBM* and *HBB*) in AAVS1 (top panel) and ATRX KO (bottom panel) samples, coloured by the expression level of DNA damage response factor UIMC1, showing the affected ATRX KO subpopulation expressing high *UMIC1*.

Supplementary Fig. 4: Characterisation of the ATRX degron cell line.

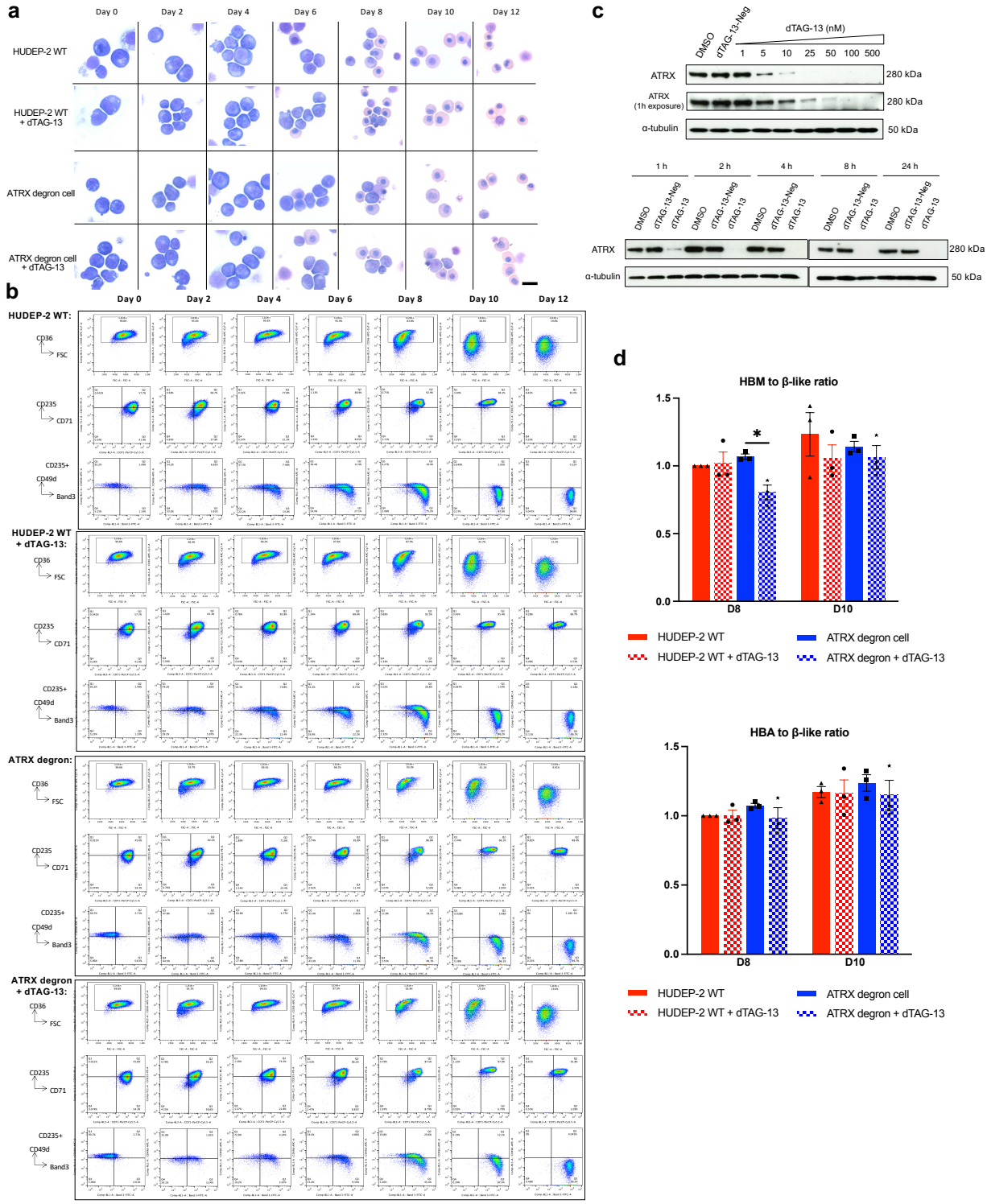

a Cellular morphology during erythroid differentiation. ATRX degron cells exhibit similar erythroid differentiation to ATRX degron cells, both with or without dTAG-13 treatment. Scale bar = 10 µm. The experiment was independently repeated at least three times with similar results. **b** Flow cytometric analysis of cell surface markers throughout differentiation, demonstrating a similar differentiation among the different groups. The experiment was independently repeated at least three times with similar results. **c** Western blot analysis of ATRX expression in ATRX degron cells. (top) ATRX degron cells treated with 0.1% DMSO,

500 nM dTAG-13-Neg, or different concentrations of dTAG-13 for 24 hours. The long-exposure (1h) blot (middle panel) reveals near-complete ATRX depletion at 100 nM dTAG-13 dose. (bottom) ATRX degron cells treated with 0.1% DMSO, 500 nM dTAG-13-Neg, or 500 nM dTAG-13 for the indicated time course, indicating rapid ATRX depletion within 2 hours of treatment. The experiment was independently repeated three times with similar results. **d** Expression ratios of *HBM* or *HBA* to β-like *(HBB+HBG)* globin in day 8 and day 10 cells, showing dATG-13 significantly downregulates *HBM* and slightly reduces *HBA* expression in day 8 ATRX degron cells (n = 3 biological replicates, data represent the mean ± SEM). Comparisons between cell lines on each timepoint were performed using one-way ANOVA followed by Dunnett test. **p* = 0.0149 for *HBM* to beta-like ratio difference between ATRX degron cells and dTAG-13-treated ATRX degron cells on day 8. Source data are provided as a Source Data file.

Supplementary Fig. 5: Generation and characterisation of the ATRX degron-VNTR KO cell model.

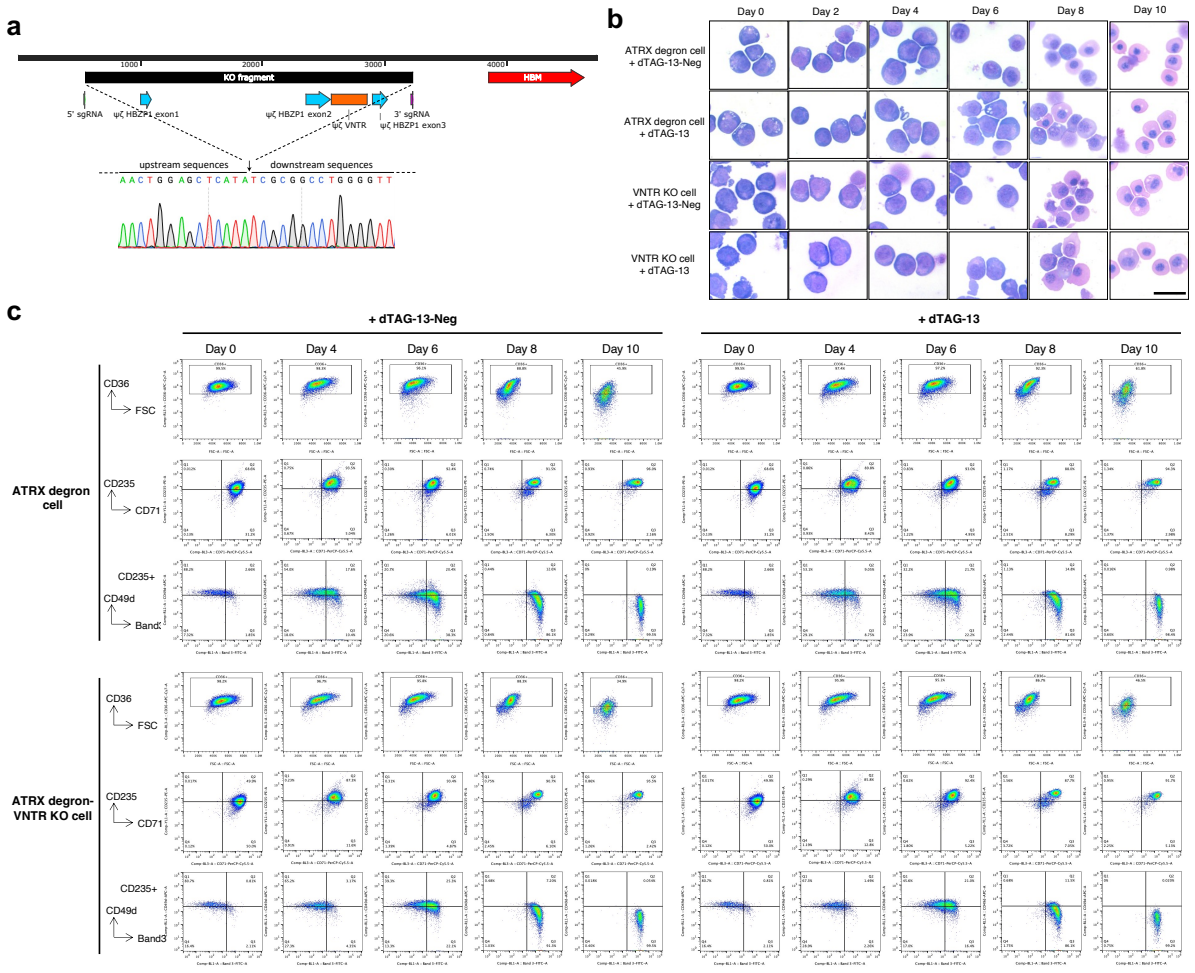

a Schematic of ψζ VNTR knockout design. The orange block represents ψζ VNTR, and the black block denotes the deleted fragment containing the entire ψζ *HBZP1,* with Sanger sequencing at the bottom confirming the homozygous deletion of ψζ VNTR. **b** Cellular morphology examination during differentiation. ATRX degron-ψζ VNTR KO cells present equivalent erythroid differentiation to ATRX degron cells, both under dTAG-13-Neg and dTAG-13 treatment. Scale bar = 10 μm. The experiment was independently repeated at least three times with similar results. **c** Flow cytometric analysis of cell surface markers during differentiation reveals similar differentiation profiles across different cells. The experiment was independently repeated at least three times with similar results.

Supplementary Fig. 6: G4 formation at the ψζ VNTR.

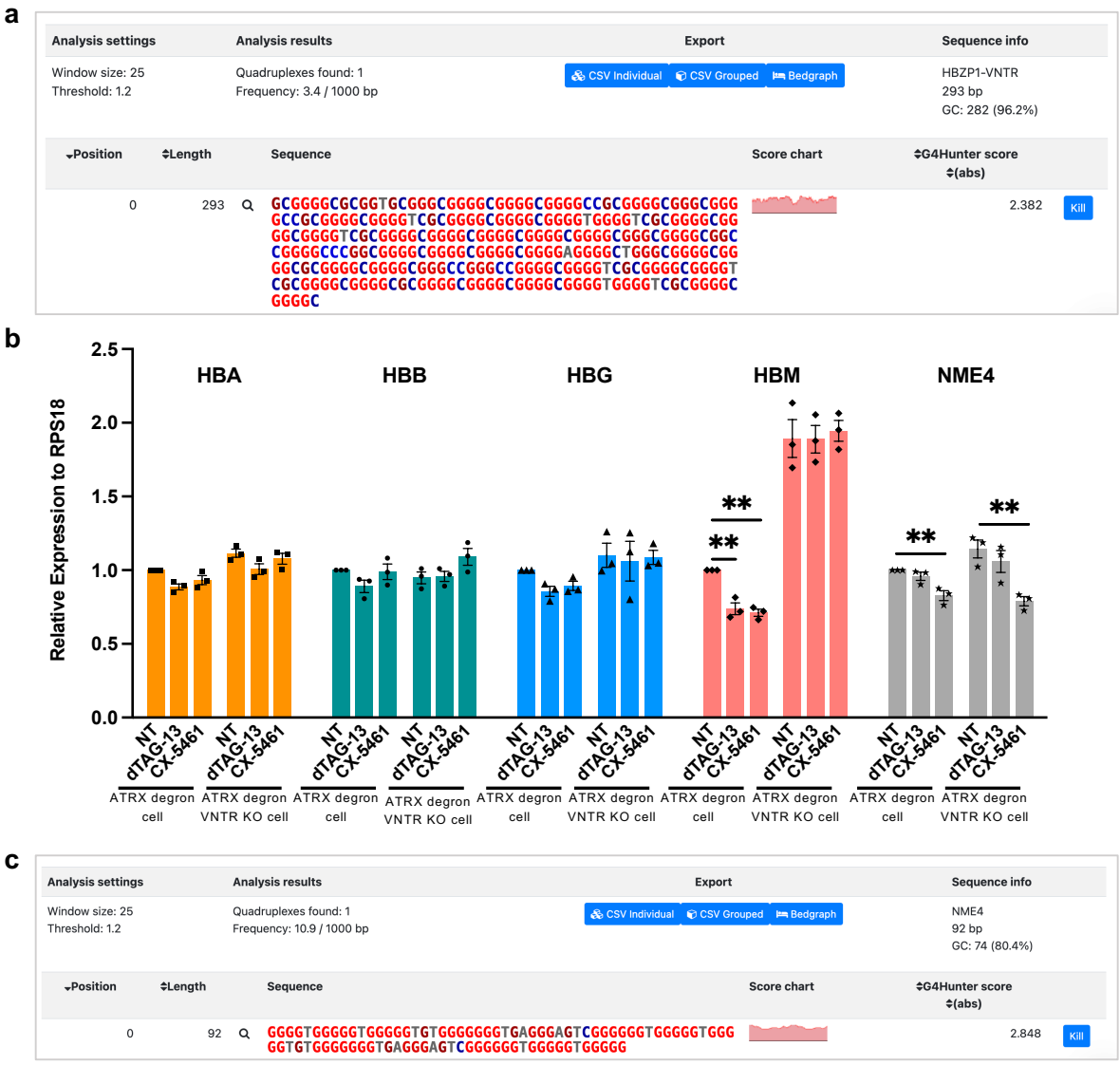

a G4 structure prediction of the ψζ VNTR sequences from reference genome GRCh38/hg38 using G4Hunter tool. A G4Hunter score > 1 indicates that a sequence is likely to form G4 structures, while a score > 2 suggests a high probability of forming highly stable G4 structures. **b** Individual gene expression (*HBA, HBB, HBG, HBM, NME4*) in day 8 ATRX degron and ATRX degron-VNTR KO cells after CX-5461 treatment. NT: untreated; dTAG-13: treated with 100 nM dTAG-13 from day 0 to day 8; CX-5461: treated with 0.1 μM CX-5461 from day 6 to day 8. For each gene, comparisons between treatment conditions within each cell line were performed using one-way ANOVA followed by Dunnett test on $\log_2$-transformed values (n = 3 biological replicates, data represent the mean ± SEM). For *HBM*, $^{**}p$ = 0.0019, 0.0010 for comparison between NT and dTAG-13, CX-5461 respectively in ATRX degron cell line. For *NME4*, $^{**}p$ = 0.0061 for comparison between NT and CX-5461 in ATRX degron cell line; $^{**}p$ = 0.0071 for comparison between NT and CX-5461 in ATRX degron VNTR KO cell line. **c** G4 structure prediction of the VNTR at *NME4* locus, showing a score of 2.848. Source data are provided as a Source Data file.

Supplementary Table 1: Sequences of guide RNAs and primers used in this study.

Purpose	Name	Sequences (5'- 3')	Target region
CRISPR sgRNAs used in CD34+ ATRX KO experiment	sgAAVS1	GGGCCACTAGGGACAGGAT	PPP1R12C
	sgATRX	GTGTAAAGACTACACCCTTG	ATRX
Genotyping primers for ATRX KO in CD34+ cells	ATRX-E9F	GAGAAATGTGGACTTGGACAGG	ATRX
	ATRX-E9R	CTTTCCCCGCCTGAGTCTTT	
gRNAs used for the generation of HUDEP-2 ATRX degron cell line	ATRX degron-gRNA	ACATTGATTTCCCTTGGGA	CTD of ATRX
Primers for ATRX degron line clonal screening	ATRX degron-F	TAGTTAATCAGCTGTGTTCAGCG	Unedited clone: 417 bp; Edited clone: 1464 bp
	ATRX degron-R	TAAAACTAATATGGAAGATTGGC	
gRNAs used for the generation of VNTR KO	VNTR-KO-sg 5'	GCAAACTGGAGCTCATAAGG	5' of HBZP1
	VNTR-KO-sg 3'	GGTCGTCCCCACTGTCGTCG	3' of HBZP1
Primers for VNTR KO line clonal screening	VNTR-KO-F1	TCACCTTCTGTGAGGAGTCCG	Unedited clone: 3119 bp; Edited clone: 438 bp,
	VNTR-KO-R	AGCCCCGACACGCTTCCAATACG	
	VNTR-KO-F2	CAAGACCTACTTCCCGCACTTC	Heterozygous KO clone: 1059 bp; homozygous KO clone: no amplification
	VNTR-KO-R	AGCCCCGACACGCTTCCAATACG	
PCR amplification of HBZP1 cDNA	Fwd	GAGCAGGCCCAACTCCAGTGC	
	HBZ+HBZP1_Rev	CGGCGCTCAGCGGTACTTCTC	HBZ (ζ-globin) HBZP1 (ψζ-globin)
	HBZ-1_Rev	ATTGGTTTATTGGCGCATTAC	HBZ (ζ-globin)
	HBZ-2_Rev	CTGGGGAACCTCCAGGAC	HBZ (ζ-globin)
	HBZP1_Rev	GGCAGGAACTGTGGGAGGGTGA	HBZP1 (ψζ-globin)
sgRNAs used for CRISPR-induced DNA damage in VNTR KO cells	sgAAVS1	GGGCCACTAGGGACAGGAT	PPP1R12C
	sgRNA-1	GCAAACTGGAGCTCATATCG	623 bp upstream of HBM
	sgRNA-2	AGCGTATTGGAAGCGTGTCG	421 bp upstream of HBM
	sgRNA-3	GAGCAGTAACTTTACCCGAG	242 bp upstream of HBM
qPCR primers for DRIP sample	VNTR-qF	CCACAGTTCCTGCCCTGACTCC	Around ψζVNTR
	VNTR-qR	TCTCCCCTCCTTCCCTCCAATAC	
	Distal region-qF	GAGATGCTGGAGTCAGGACCAT	A distal region on chr16
	Distal region-qR	AGGAGTCAGGAGCAGCAGTCA	

Supplementary Table 2: Flow antibodies used in this study

	Protein Marker	Color	Manufacturer	Cat No	Dilution
Erythroid differentiation panel (for both CD34+ and HUDEP-2 cells)	CD34	PE/Cy7	Biolegend	343616	1:100
	CD36	APC/Cy7	Biolegend	336213	1:100
	CD71	PerCP/Cy5.5	Biolegend	334114	1:100
	CD235a	PE	BD Bioscience	555570	1:100
	CD49D	APC	BD Bioscience	561892	1:100
	CD233 (Band3)	FITC	IBGRL	9439FI	1:100
	Hoechst 33258	violet	Invitrogen	H3569	1:10000
Haematopoietic progenitor cell panel for CD34+ cells	CD34	PE/Cy7	Biolegend	343616	1:100
	Lineage cocktail (CD 2/3/56/14/16/19/235a)	APC	Thermo Fisher Scientific	22-7776-72	1:33
	CD36	PerCP/Cy5.5	Biolegend	336223	1:50
	CD71	FITC	eBioscience	11-0719-41	1:20
	CD41a	EF450	eBioscience	48-0419-41	1:50
	CD105	PE	Biolegend	323205	1:50
	CD38	AlexaFlour 700	Biolegend	303523	1:50
	CD45RA	APC-eFluor 780	eBioscience	47-0458-41	1:50
	CD123	BV605	BD Bioscience	564197	1:12.5
	CD90	BV711	BD Bioscience	740786	1:20
	CD10	APC	eBioscience	17-0106-42	1:20
	Fixable Viability	BV510	BD Horizon	564406	1 µL per 1 mL